Materials Chemistry and Physics 260 (2021) 124163

Contents lists available at ScienceDirect

Materials Chemistry and Physics

journal homepage: www.elsevier.com/locate/matchemphys

Optimization aspects of electrodeposition of photoluminescent conductive polymer layer onto neural microelectrode arrays

T. Marek [a,*], G. Orbán [b,c], D. Meszéna [b,d], G. Márton [b,c,d], I. Ulbert [b,d], G. Mészáros [a], Z. Keresztes [a]

[a] Functional Interfaces Research Group, Institute of Materials and Environmental Chemistry, Research Centre for Natural Sciences, Budapest, Hungary
[b] Comparative Psychophysiology Research Group, Institute of Cognitive Neuroscience and Psychology, Research Centre for Natural Sciences, Budapest, Hungary
[c] Doctoral School on Materials Sciences and Technologies, Óbuda University, Budapest, Hungary
[d] Faculty of Information Technology and Bionics, Pázmány Péter Catholic University, Budapest, Hungary

HIGHLIGHTS

- Photoluminescent, conductive PEDOT layer can be deposited on neural microelectrode arrays by direct electropolymerization.
- The structure of PEDOT layer can be controlled by the number, length and voltage of electric pulses applied in the process.
- Optimization of applied monomer concentration is important to avoid the formation of detached polymer particles.
- $BMIMBF_4$ ionic liquid is a better electrolyte for the polymerization process than $PC(LiClO_4)$.

GRAPHICAL ABSTRACT

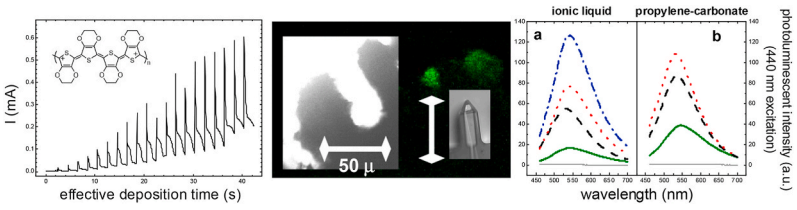

ARTICLE INFO

Keywords:
Neural microelectrode
Conductive polymer
PEDOT
Photoluminescence
Direct electropolymerization

ABSTRACT

In neuroscience the use of a microelectrode array allows the detection of neuroelectric signals with high temporal resolution in a confined space within the tissue, while two-photon laser scanning microscopy provides high spatial resolution in a wide region of interest. The combination of these two techniques promises better understanding of the operation of neural pathways. To facilitate this connection, we studied the direct electrochemical deposition of the conductive polymer poly-2,3-ethylenedioxy-thiophene onto different Pt and Pt/Ir electrode surfaces from non-aqueous solvents, such as ionic liquid and propylene carbonate. We show the effects of electrochemical deposition technique (pulsed or continuous), monomer concentration range and solvent electrolyte type on the formation of photoluminescent - conductive films. For these variables we determined the optimal deposition parameters given as 0.025–0.050 M EDOT monomer concentration in $BMIMBF_4$ ionic liquid and the use of pulsed deposition process to form an adherent, uniform functional electrode coating.

* Corresponding author.
E-mail address: marek.tamas@ttk.hu (T. Marek).

https://doi.org/10.1016/j.matchemphys.2020.124163
Received 16 July 2020; Received in revised form 8 December 2020; Accepted 10 December 2020
Available online 14 December 2020

1. Introduction

The operation of neural pathways is based on transmission of chemical and electric signals and understanding this communication requires specific tools to record and conceive the signals. For recording these small electric signals several reliable methods and electrode systems have been developed. The main goal of these advancements was to minimize the size of the electrode, thus reducing the geometric area of the potential recording sites for minimizing the brain tissue injury and for better allocation of the signal source. A step in the refinement of the spatial resolution is the use of spatially linked electrodes and studying the correlation between the observed electric signals on the individual electrode sites. The multi-channel laminar platinum-probe array (referred thereinafter as "SPIKY" from "spiky probe") [1,2] used in this study is such device, designed for *in vitro* slice recordings.

Two-photon laser scanning microscopy (2PLSM) is a fluorescent imaging technique based on the physical effect of two-photon (2P) excitation, where the principle is the addition of two UV photons into one fluorescent excitation. Today, 2P imaging is a widely used complementary technique besides electrophysiology for the acquisition of neural activity with single-cell resolution from hundreds of neurons both *in vitro* and *in vivo* [3]. While fluorescent microscopy only provided static (or structural) information of the investigated tissue via 'green fluorescent protein' (GFP) based fluorescence, 2PLSM more recently allowed for functional imaging and tracking physiological processes almost in real time [4]. In 2P microscopy, all emitted photons are useful, that dramatically increase the signal-to-noise ratio, unlike in the case of confocal microscopy, where scattered photons are rejected. As a consequence, photodamage and bleaching is greatly reduced, since the probability of fluorophore excitation depends quadratically on light intensity, rather than linearly as in the case of confocal fluorescence. Generally, single-photon imaging techniques use fluorophores that are activated in the 400–500 nm (visible) wavelength range, for 2P excitation this range falls into the near-infrared (NIR) ranges (between 700 and 1300 nm) resulting in a higher possible penetration capability. Lower energy, longer wavelength excitation is rather suitable for *in vivo* and chronic imaging of living animals, as it causes less phototoxicity.

It is known that extracellular electrophysiology and 2P imaging both have advantages and disadvantages in sense of spatial or temporal resolution and structural or functional information extracted. The idea to combine them comes naturally to gain maximal benefit from both techniques. Initial attempts to integrate the two modalities, however faced the phenomenon called 'photoelectric artefact' that interferes with electronics and thus can contaminate (or even prevent) simultaneous extracellular recordings if the Field-of-View of imaging includes the recording sites of the solid-state multielectrode [5]. Several strategies have been used to avoid photoelectric effects, such as the use of transparent probe materials or ionic conductors (e.g. glass pipettes) or attenuation of the generated artefact via specifically designed filtering algorithms but each of these approaches has its own limitations [2,6,7]. Nevertheless, if co-localized extracellular recording and 2P imaging is elaborated, subsequent, although not synchronous recordings can be achieved without photoelectric contamination.

The basic use of fluorescent markers in 2PLSM is used to assign the individual neural cells. To localize individual electrode sites at the same time, the electrode marking material has to be also photoluminescent. It has been shown that poly-3,4-ethylenedioxy-thiophene (PEDOT) can show such behavior [8]. PEDOT is a conducting polymer with an extremely wide-spread literature. The concise book of Elschner [9] contains not only data from the literature but so far unpublished results as well. PEDOT combination with the polyanion poly-styrene-sulfonate (PEDOT:PSS) exists in aqueous suspension forms so it can be used for the formation of conductive layers by conventional wet methods, such as dip coating or spin coating ready to be used in combined electronic applications [10]. For the modification of the SPIKY tips the PEDOT:PSS composition is inadequate, since the electrode coating is to be contacted with the organic tissue, thus its quality is subject of deterioration in such an aqueous environment.

Direct electrodeposition process is a feasible technique to form spatially directed coatings on conducting surfaces. Márton et al. has shown that an adherent high surface area Pt layer could be formed on microelectrode surfaces by electrodeposition [11].

As an alternative surface modification process, Prasad et al. [8] have formed PEDOT particles polymerized on indium-tin-oxide (ITO) electrode with 1-butyl-3-methylimidazolium-tetraflouroborate ($BMImBF_4$) as non-aqueous electrolyte. Alternatives of non-aqueous ionic liquid (IL) electrolyte, such as propylene-carbonate (PC) have been already used [12]. It is a lower cost material, but as the physical properties of the electrodeposited PEDOT are very dependant on the properties of the growth solvent [13], hence its use is not beneficial in every case. The solvent dependence is due not only the difference in the incorporated ("doping") anions, but also the different nucleation mechanisms and morphologies. The related literature is complex in respect of variables and difficult to compare. Sandoval et al. [14] used IL, but with different anion and galvanostatic deposition process, Cysewska et al. [15] applied acetonitrile as solvent electrolyte for potentiostatic and galvanostatic deposition, while in the paper of Suominen et al. [16] again IL and acetonitrile was used, but the difference in the method of deposition, namely potentiodynamic cycling makes the comparison of results difficult.

The phenomena of photoluminescence (PL) of PEDOT layer is not fully understood yet. Ivanko et al. assign PL to structural causes, as a result of water incorporated into the "bulk" PEDOT [17]. Prasad et al. explain the PL of the PEDOT by the assumption of the presence of quantum dots [8]. But there is a significant difference in the preparation methods – while Prasad et al. use electrochemical deposition from IL, the group of Ivanko uses chemical oxidation and aqueous solution, which explains the incorporated water, but leaves somewhat open the question of the origin of PL.

In this work we show our results on direct electrodeposition of photoluminescent PEDOT coatings onto neural microelectrodes and the optimization of the process in respect of used electrodeposition technique, monomer concentration and solvent electrolyte type. The novelty of the results is the development of an easy, one-step, dual-role surface modification procedure, which results in an electrode coating that not only maintains conductivity and provides high surface area, but also creates site specific photoluminescence as added value to help exact site localization in nerve tissue electrode systems.

2. Materials and methods

2.1. Materials

3,4-ethylenedioxy-thiophene, EDOT, as monomer (Sigma-Aldrich, 97%) was used in the electropolymerization process. Two types of electrolyte were used, the ionic liquid, IL, pure 1-butyl-3-methylimidazolium-tetraflouroborate, $BMImBF_4$, (Merck, high purity) and propylene-carbonate, PC, (Sigma-Aldrich, 99.9%, anhydrous) with added conducting salt to yield 0.1 M $LiClO_4$ ($LiClO_4{\cdot}3H_2O$, Merck, alt.). Three substrate materials were used: platinum (Pt) sheet, polyimide insulated Pt/Ir (Pt 80%, Ir 20%) wire of 40 μm diameter (California Fine Wire Company) and the electroactive tips of a neural microelectrode array ($Pt/Ir/IrO_2$, ~5 μm, SPIKY, see Introduction). The post-processing of the polymer (PEDOT) involved N,N-dimethyl-formamide (DMF, VWR Chemicals, 99,9%), water (MQ, MilliPore, 18 MΩ cm) and H_2SO_4 (Molar Chemicals, 96%, puriss.).

2.2. Electropolymerization

For the electropolymerization process we prepared two base electrolytes: One was the pure IL, the other 0.1 M $LiClO_4$ in PC (prepared by dissolving 160.4 mg $LiClO_4{\cdot}3H_2O$ in 10 cm^3-s of PC). Using these, 0.1 M

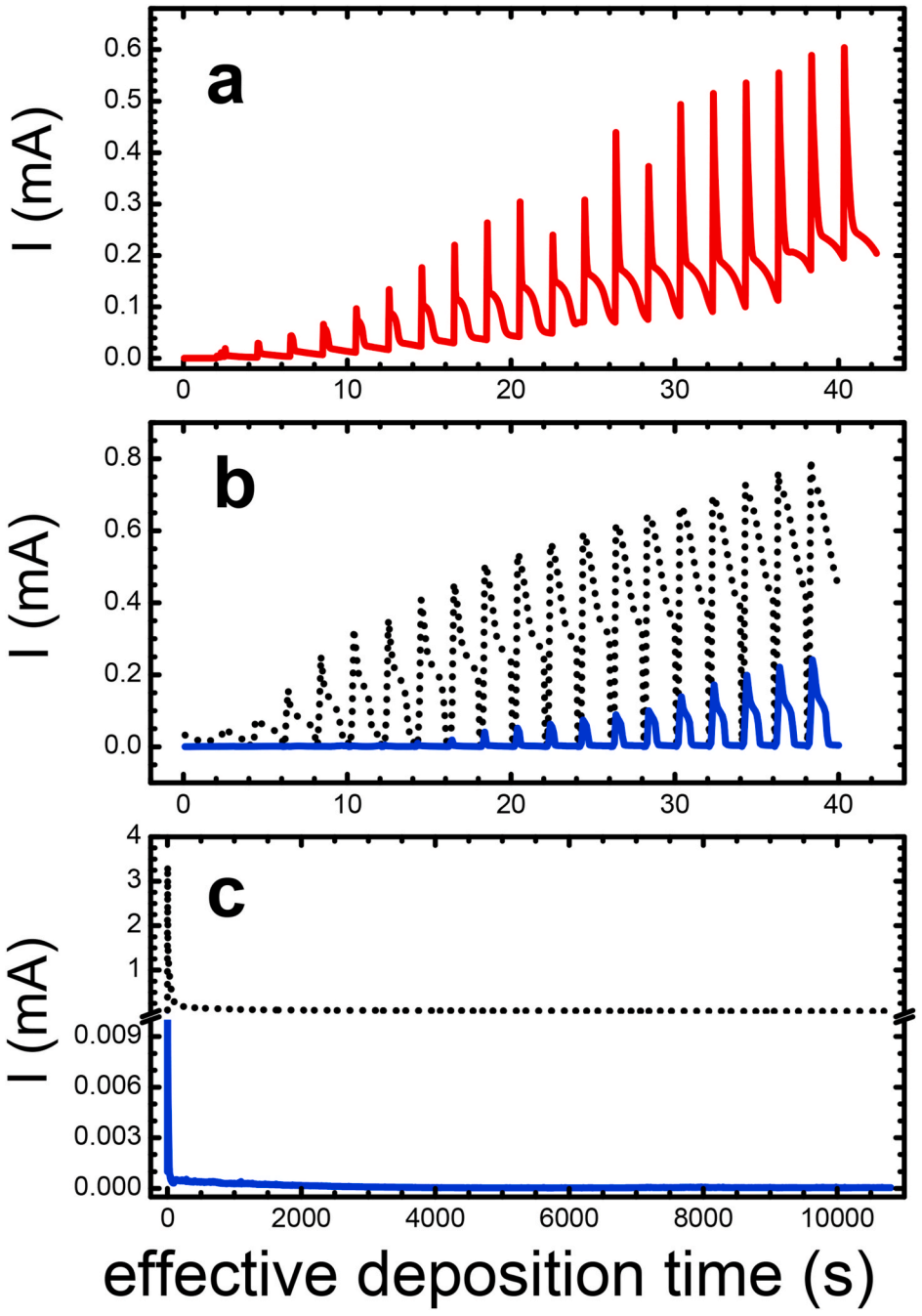

Fig. 1. Different observed effective chronoamperometric curves of the PEDOT electrodeposition to different substrates: a) microelectrode array tip, b) and c) Pt/Ir wire. Sections a) and b) show the characteristic I(t) curves during the on-states of the pulsed deposition and c) during continuous (potentiostatic) deposition. Solid curves correspond to depositions only to the tips of insulated wire, while dotted curves show the depositions to the non-insulated wire (both tip and side).

EDOT solutions were prepared (by adding 11 μL of EDOT to 989 μL solvent (PC with $LiClO_4$, or IL). The final dilution step was performed just before the polymerization to yield 0.025 M EDOT solutions in PC for all the small-area electropolymerization processes; for the high-area electrodes 0.010 M, 0.025 M and 0.050 M EDOT solutions both in PC and IL were used. In the case of IL the original 0.1 M EDOT solution was also added to the series.

There were small-area and large-area substrates. The formers are the tips of the multichannel array as well as the tip of the model Pt/Ir wire. The wire tip was prepared by the cross-cutting the wire, with no further polishing; hence the surface areas of these tips were somewhat different. The large-area substrates are the Pt sheet and the cylindrical side of the Pt/Ir wire with removed insulation. The insulating polyimide layer has been removed by a butane flame. As the surface area of the "tip&side" (non-insulated) wire samples was difficult to determine, the currents were not normalized by the area.

All electropolymerization experiments have been conducted in a non-thermostated open-to-air cylindrical cell of 9 mm diameter containing 0.4 cm^3 non-stirred electrolyte. Usually all the electrodes (the Pt wire coil counter electrode (CE), the Ag-wire quasi-reference electrode (RE) and the substrate as working electrode (WE)) were submerged in the electrolyte from the top. In the case when the substrate was a Pt sheet, it replaced the bottom of the cell.

For the large-area substrates simple potentiostatic deposition was performed with a long, 3 h deposition time at 1.5 V using an Autolab PGSTAT124 N potentiostat; during deposition current is recorded

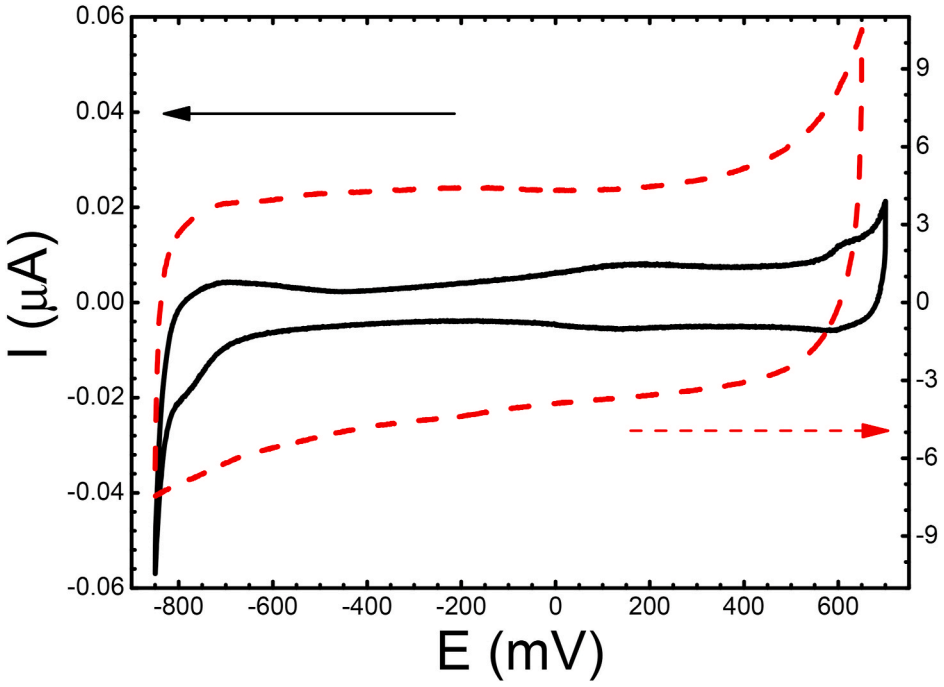

Fig. 2. Characteristic monitoring CVs of a microelectrode array tip before and after the deposition of PEDOT layer (0.5 M H_2SO_4, 0.5 V/s sweep rate, RE-CE: common Pt-wire, WE: tip). The left-hand side scale corresponds to the solid curve of the pristine electrode tip, the right-hand side scale to the dashed curve recorded after PEDOT deposition.

yielding chronoamperometric curves.

For the small-area substrates (SPIKY and wire tips) pulsed deposition was performed to avoid the formation of oversized PEDOT parts. This pulsed deposition was a series of 30 s cycles, which cycles started with a potential pulse, on-state, with varying amplitude (1.5 and 2.0 V) and duration (1 or 2 s), and a "forced relaxation period" for the remaining time at 0 V, off-state. On the current vs. time curves of Fig. 1 only the currents during deposition are displayed, the current related to the relaxation period is disregarded.

The current source for such electropolymerization onto the small-area SPIKY tips was a custom made bipotentiostat [18] which provided low-noise current measurements even in the pA current range, the cell was in a Faraday-cage.

2.3. Post-polymerization processes

The PEDOT films deposited onto the small-area substrates (SPIKY tips and thin wires) were rinsed and three times ultrasonicated in MQ water.

The conductivity of the SPIKY tips was monitored by taking cyclic voltammograms (in 0.1 M H_2SO_4 water, −850 to 600 mV vs. common Pt-wire CE and quasi-reference electrode; the sweep rate 500 mV/s) before and after deposition.

2.4. Formation of photoluminescent PEDOT

In order to study the efficiency and controllability of PEDOT layer formation the overall quantity of polymerized PEDOT was to be determined. The Pt-sheet deposition experiments resulted in not only adhered PEDOT layer but also dispersed PEDOT particles, and the total amount was to be accounted for the polymerization process. To follow the efficiency of deposition the samples were treated as follows. The electrolyte was removed from the cell, and the surface of the PEDOT-covered Pt-sheet was gently rinsed by 3 × 200 μL MQ water. This rinsing water and the electrolyte was then mixed in an Eppendorf vial, ultrasonicated for 2 min and then centrifuged for 30 min at RT and 15,000 rpm. The liquid fraction was then disposed, the remaining particles were left to dry overnight, just as the PEDOT-covered Pt-sheet. The dried PEDOT from the Pt-sheet was scraped off first into a glass weighing boat then transferred to an Eppendorf vial. The electrolyte- and Pt-sheet-origin PEDOT were then treated the same way. The dried samples were dispersed in 1 cm^3 MQ water, and were ultrasonicated for 2 min and then centrifuged for 30 min at RT and 15,000 rpm. The supernatant was then disposed, and this cleaning process was repeated three times. The sample was dried and the weight was measured.

The photoluminescence (PL) of the PEDOT samples was studied in DMF suspension. 1.2 cm^3 DMF is added to the dried samples and ultrasonicated for 4 h at 30 °C, then centrifuged for 45 min at 15,000 rpm and 20 °C. For further studies the suspension was used. The PL spectra are recorded by a Thermo Scientific VarioScan Flash plate reader between 460 and 700 nm with a 440 nm excitation wavelength, using 290 μLs of the samples measured into standard 96-well flat-bottom polypropylene plates at RT.

To avoid the high level of uncertainty introduced by the small amount of materials we show the averaged results of five parallel high-area deposition experiments together with their standard deviations for all electrolytes and concentrations.

2.5. Microscopy techniques

The two-photon microscopic (2P) laser scanning pictures and the optical pictures of the SPIKY multielectrode array were both recorded by the microscope of the Group of Comparative Psychophysiology, ICNP, RCNS. The *in vitro* 2P recording set-up was built on the base of an Olympus BX61 upright microscope by Femtonics Ltd. (Femtonics Ltd., Budapest, Hungary) and has a near-infra red (NIR) bright-field camera mode as well as a 2P fluorescent working mode. For the 2P excitation, a Ti:Sapphire femtosecond pulse laser was used (Coherent Chameleon Ultra II, Coherent Inc., Santa Clara, CA, USA) with a chosen wavelength of 800 nm. The laser can yield a maximal output intensity of 4 W at 800 nm wavelength, which finally results in a measured maximally power of 1 W after the last optical element (objective lens) at the focal point. This

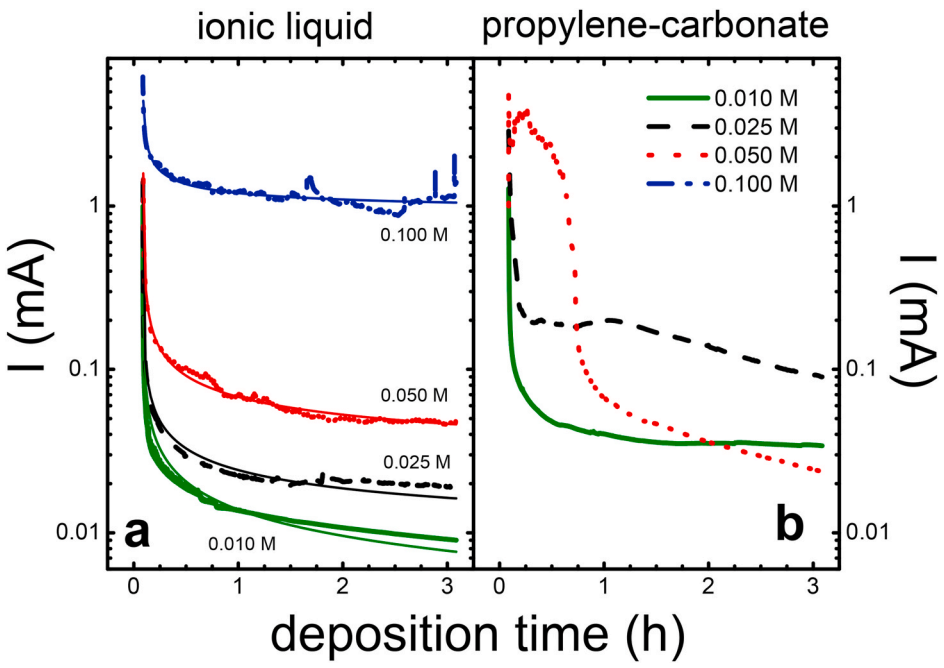

Fig. 3. Averaged chronoamperometric curves of potentiostatic PEDOT electrodeposition from a) ionic liquid and b) propylene-carbonate electrolytes with different monomer concentration. The thin lines in panel a) are fits of the Cottrell-equation.

power would be enough for imaging the neural tissue and its activity in a depth of hundreds of μm or even up to 1 mm. In the case of the floating wires, we have set the imaging laser intensity to 10–15% (100 mW) and the sensitivity of the green photomultiplier (PMT) detector to 50%. Scanning was carried out in resonant raster scanning mode. We used a water immersive 20x objective (Olympus, XLUMPLFLN20XW) with a numerical aperture of 1 and a working distance of 2 mm. Recorded images were pre-processed and exported using the integrated software package of the Femtonics microscope system.

The simple optical microscopic pictures of the wire were recorded by a CCD camera attached to an Optech (Optech GmbH, Germany) stereomicroscope.

3. Results and discussion

3.1. Characteristic electrochemical parameters of PEDOT deposition process

Fig. 1 shows effective chronoamperometric curves observed during PEDOT deposition experiments.

In the I(t) curves of Fig. 1 panels a) and b) the effective deposition process is represented by the data when the WE (substrate) was on non-zero potential, on-state, the continuity achieved by editing out the off-state data (E = 0 V) and the deposition pulses shifted immediately behind each other (see 2.2). Fig. 1b) and c) refer to results of the pulsed and continuous deposition experiments, b) and c) respectively, carried out on the wire substrates. Note that the initial parts of all deposition cycles are similar to the initial part of the continuous deposition curve, clearly signaling the same electrochemical behavior. The 2-s pulse length deposition curves (Fig. 1a.) show the increase of the total charge by repetition of the deposition pulse, indicating the increasing surface area of the electrode, i.e. the deposition of additional PEDOT. Fig. 1b shows that the pulsed deposition strategy also works for substrates with slightly different composition and increased surface areas, as on the wire substrates. As it can be seen, the area difference of the tip and tip-and-side surfaces manifests again in the deposition currents (and charges). Finally, Fig. 1c shows that this difference is also present when the polymerization is conducted by a long-term continuous potentiostatic strategy.

As a monitoring method, cyclic voltammetry was used to assure the quality of the original, pristine electrodes surfaces and to compare the conductivities of the sites before and after the deposition process. First, we examined the quality of the individual SPIKY sites, whether they comply the needs of the deposition experiments: their surface areas are same, they are not contaminated/blocked and the overall resistance is similar. The aim of the post-deposition CVs was to compare the conductivities of the pristine and the covered sites. In order to simplify the experimental setup, we chose to use 0.5 M H_2SO_4 as electrolyte for the CVs and a two-electrode system, where the working electrode was the actual SPIKY site and the Pt-wire counter-electrode acted as a quasi-reference electrode. As the surface areas and currents were low and the measurement times short, the use of such quasi-reference electrode is valid.

On Fig. 2 the CV recorded on a pristine site of the SPIKY array shows great similarity to typical CVs recorded on Pt surfaces in dilute aqueous acid under ambient atmosphere. The peaks correspond to surface adsorption-desorption processes present on Pt surface in aqueous solution [11]. The CV shown on Fig. 2 by dashed line shows that after PEDOT deposition the surface remained conductive. The surface modification resulted in a CV of boxlike form of an electrochemical double-layer capacitor [19]. The deviations from the shape expected from an ideal capacitor are due to the high internal resistance of the electrode and parasitic reactions. It should be noted that the measured currents are two orders of magnitude higher than the pristine values, presumably as the result of the increased surface area of the site.

These results above showed that the deposition of the conducting polymer layer was successful, and the characteristic features of the pulsed or continuous deposition curves can be used for monitoring the process. By decreasing the length of the deposition pulse one can have a better control over the thickness of the formed layer.

3.2. Solvent-type and monomer concentration dependence of PEDOT deposition

As the electrolyte choice was proven to be important in the quality of the deposited polymer, we selected two types of electrolytes represented

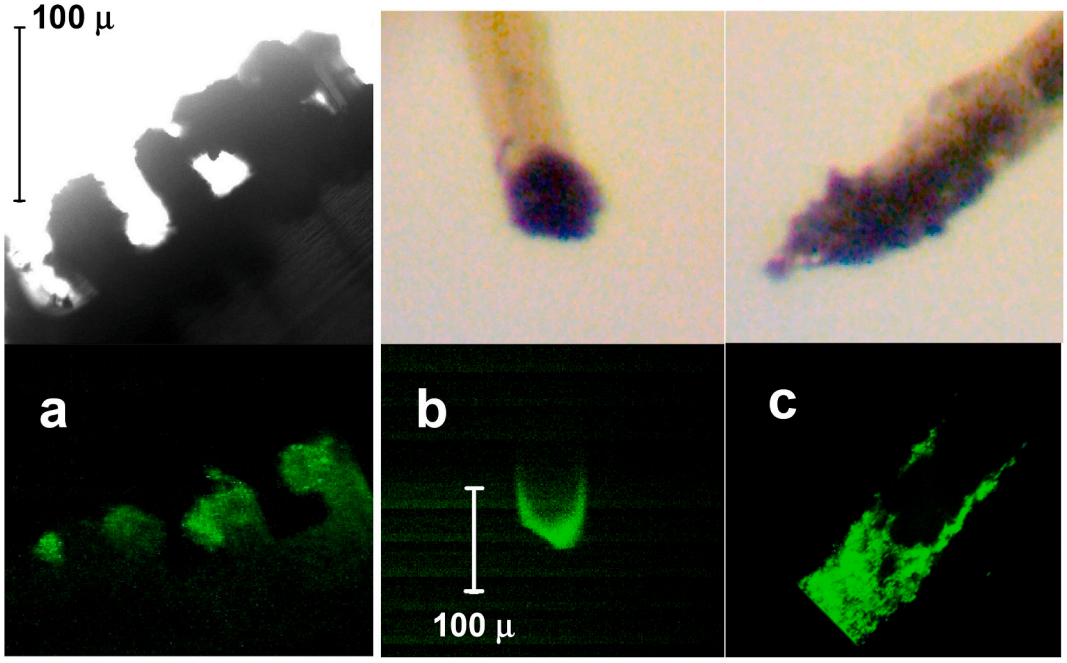

Fig. 4. Optical (top) and two-photon microscopic (bottom) photos of the cleaned PEDOT deposited onto a) microelectrode array tips, b) Pt/Ir wire tip and c) side.

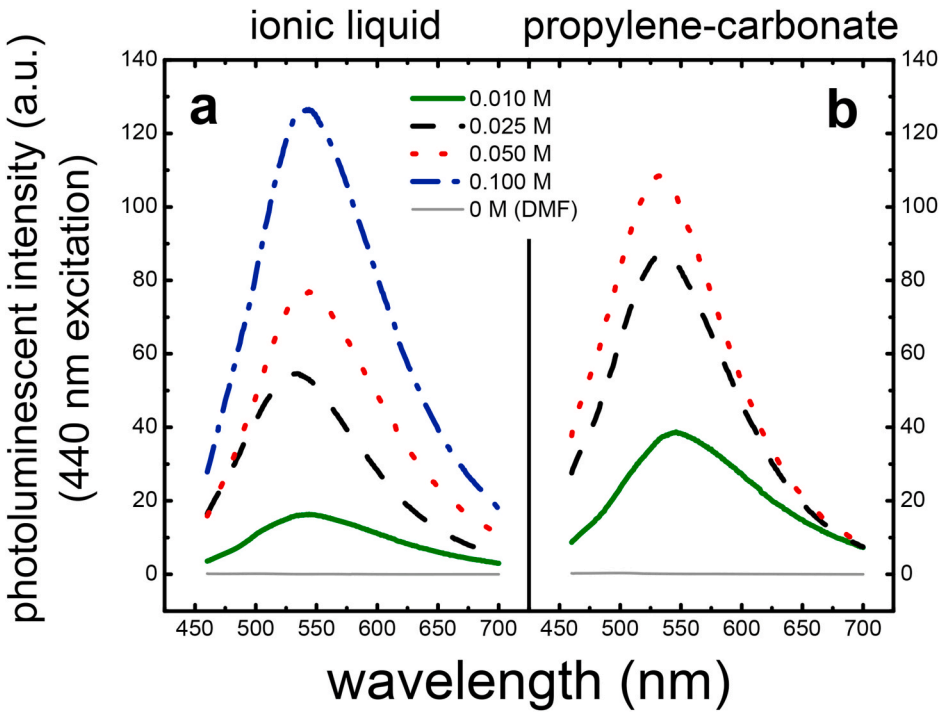

Fig. 5. Summed and averaged photoluminescence spectra (λ_{ex} 440 nm) of the DMF-suspended PEDOT particles deposited from a) IL or b) PC with different EDOT-content.

in the literature for this task previously [8,12]. We used propylene-carbonate (PC) based electrolyte and pure 1-butyl-3-methylimidazolium-tetraflouroborate ($BMImBF_4$), which is an ionic liquid (IL), with inherently good conductivity and similar density as PC, but with a slightly higher apparent viscosity. We have also determined whether there is an optimum concentration for the monomer (EDOT) so we conducted long-term potentiostatic electrodeposition experiments from electrolytes with different EDOT-concentrations and chemical composition. The deposition currents of these experiments are shown on Fig. 3. Each data set represents the average of five parallel measurements. The drawback of PC as solvent is apparent, the I(t) curves that follow the deposition process are much less regular than those observed in IL. These results show that the use of curves obtained in PC solvent are far not optimal for following the individual deposition processes. On the other hand, the deposition curves recorded in IL show mainly pure diffusional behavior, as shown by the fitted theoretical Cottrell-curves.

The original Cottrell-equation connects the time elapsed after a potential step and the responding current in the case of a planar electrode

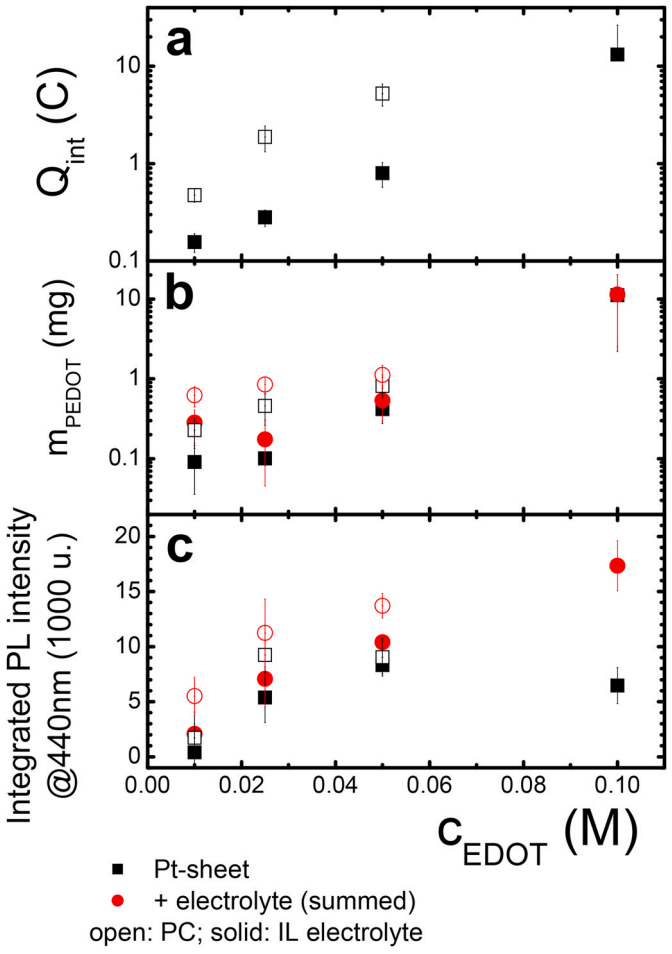

Fig. 6. Integral parameters of the PEDOT-deposition as a function of solvent type and the monomer concentration. a) shows the total observed charge during the 3 h deposition process, b) is the measured mass of the deposited PEDOT onto the Pt-sheet (squares) together with the total mass, corrected with the polymer-content of the electrolyte (circles), c) is the integrated photoluminescence of the PEDOT-dispersions (squares and circles are the same as in panel b)). In all of the figure open and solid symbols represent PC and IL electrolytes, respectively, the error bars denote the standard deviations from five parallel deposition experiments.

and purely diffusional matter transport, described *e.g.* in Bard & Faulkner [20]. The formation of PEDOT particles on the surface of the Pt-sheet is consistent with this picture, while the time range of these experiments is well out of the usual time range of the clear diffusional regime [21,22].

It is also important to note that in the case of PC the highest EDOT concentration applicable was lower than in IL. It was because even at 0.050 M EDOT concentration the potentiostatic condition could only just fulfilled, this way compromising the site specificity of deposition reaction.

The representative optical and two-photon microscopic pictures of the PEDOT layers deposited onto small-area substrates (Fig. 4.) reveal that while the conductive and photoluminescent coating is achieved on all substrates, the quality of these coatings is not uniform. The main possible problem is observable on Fig. 3a, where the deposited PEDOT grows in cauliflower-type form and can connect neighboring sites.

This behavior showed the need for a better control over the deposition process. The use of a large-area substrate, Pt-sheet, allowed us to gain insight into the reproducibility and controllability of this process, using higher amounts of material. Fig. 5 shows derived luminescence spectra of the PEDOT particles deposited on Pt sheet. These spectra show the same features as in Ref. [8], indicating the same final composition and structure. Moreover, the observed PL intensities reflect the PEDOT concentration quite well [8].

The PEDOT samples were electrodeposited from the corresponding electrolyte, then removed from the Pt-sheet substrate, cleaned, and resuspended in DMF as described in 2.4. The photoluminescence (PL) spectra were recorded in this suspension. The obtained intensity values can be treated representative for the PEDOT concentration. The curves shown are obtained by summing the PL spectra of the PEDOT removed from the Pt-sheet and extracted from the electrolyte for each individual deposition experiment and averaged for a given electrolyte-concentration pair.

The comparison between the electrolytes and concentration ranges is the simplest by the aid of integrated measures. One such measure is the total charge, Q during the deposition, the mass of the formed PEDOT and the PL-intensity, which is chosen simply as the total area under the spectra shown on Fig. 5.

The comparison of these integrated measures is shown on Fig. 6. Mark that at panels b) and c), mass and intensity, respectively, we have shown the values obtained for the PEDOT originating from the Pt-sheet only and the total amount of PEDOT ("summed"). The error bars shown are the standard deviation of the data. It is very interesting to see that all integrated measures show that at any given monomer concentration it is possible to produce more PEDOT from PC than from IL solvent. It can be speculated that this is the consequence of the lower viscosity, and higher reaction rate due to the higher diffusion rate. On the other hand, the gap between the deposited and total amount of PEDOT also increases with the increasing EDOT-concentration, meaning that less and less of the PEDOT covers the substrate. The size of this gap is lower for the IL electrolyte in the whole concentration range, which means stronger control over the formed PEDOT.

Based on the data shown on Fig. 6, the optimal electrolyte composition for the PEDOT deposition is in the 0.025–0.050 M EDOT in IL. Optimization of applied EDOT-concentration is crucial, as in the lower EDOT-concentration region the deposited polymer is scarce and its quantity is quite uncertain, but in higher concentration of PEDOT is not necessarily adheres to the surface. The presence of detached, surplus PEDOT in the electrolyte could also contaminate those parts of the substrate which should remain intact and cause undesirable short circuits and other side effects.

4. Conclusions

The results presented in this work show the feasibility of direct electrochemical deposition of photoluminescent PEDOT layer onto conducting substrates. The method can be used to modify neural recording electrodes to allow spatial localization of bioelectric signals in nerve tissue. This way a dual detection platform can be fabricated with the combination of conductivity and photoluminescence functions.

Well-controlled good quality coating preparation is crucial to achieve the desired functionality, as polymeric layer overgrowth can be a serious issue in the spatial resolution of the device. Fine tuning of the coverage could be controlled by using electric pulse deposition technique.

Electrolyte quality has been proven to have a strong influence on the deposited PEDOT amount. Due to the diffusion-controlled deposition observed, the ionic liquid ($BMImBF_4$) solvent is a better choice for layer preparation than propylene-carbonate/$LiClO_4$. The obtained monomer concentration dependencies on the other hand show that to handle the deposition process one has to optimize monomer concentrations, which is in our case in the range of 0.025–0.050 M EDOT.

Further optimization of the pulsed deposition technique (pulse length, number and voltage, monomer concentration) in ionic liquid as electrolyte is in progress.

CRediT authorship contribution statement

T. Marek: Conceptualization, Methodology, Investigation, experiments, Data curation, Visualization, Formal analysis, Writing - original draft, Writing - review & editing. **G. Orbán:** experiments, Data curation, Visualization. **D. Meszéna:** Investigation, experiments, Visualization, Writing - original draft, Writing - review & editing. **G. Márton:** Conceptualization, Methodology, experiments, Writing - review & editing, Funding acquisition. **I. Ulbert:** Conceptualization, Methodology, Writing - review & editing, Funding acquisition. **G. Mészáros:** Conceptualization, Methodology, Investigation, experiments. **Z. Keresztes:** Conceptualization, Methodology, Writing - original draft, Writing - review & editing, Funding acquisition.

Declaration of competing interest

The authors declare that they have no known competing financial interests or personal relationships that could have appeared to influence the work reported in this paper.

Acknowledgements

Financial support of BIONANO GINOP-2.3.2-15-2016-00017 and VEKOP-2.3.2-16-2017-00013 by the European Union and the State of Hungary, co-financed by the European Regional Development Fund are gratefully acknowledged.

References

[1] D. Meszéna, B.P. Kerekes, I. Pál, G. Orbán, R. Fiáth, T. Holzhammer, P. Ruther, I. Ulbert, G. Márton, A silicon-based spiky probe providing improved cell accessibility for in vitro brain slice recordings, Sensor. Actuator. B Chem. 297 (2019) 126649, https://doi.org/10.1016/j.snb.2019.126649.

[2] G. Orbán, D. Meszéna, K.R. Tasnády, B. Rózsa, I. Ulbert, G. Márton, Method for spike detection from microelectrode array recordings contaminated by artifacts of simultaneous two-photon imaging, PloS One 14 (8) (2019), e0221510, https://doi.org/10.1371/journal.pone.0221510.

[3] W. Denk, J.H. Strickler, W.W. Webb, Two-photon laser scanning fluorescence microscopy, Science 248 (4951) (1990) 73.

[4] K. Svoboda, R. Yasuda, Principles of two-photon excitation microscopy and its applications to neuroscience, Neuron 50 (6) (2006) 823.

[5] T.D. Y Kozai, A. L Vazquez, Photoelectric artefact from optogenetics and imaging on microelectrodes and bioelectronics: new challenges and opportunities, J. Mater. Chem. B 3 (25) (2015) 4965.

[6] Y. Qiang, P. Artoni, K.J. Seo, S. Culaclii, V. Hogan, X. Zhao, Y. Zhong, X. Han, P.-M. Wang, Y.-K. Lo, et al., Transparent arrays of bilayer-nanomesh microelectrodes for simultaneous electrophysiology and two-photon imaging in the brain, Sci. Adv. 4 (9) (2018), eaat0626.

[7] A. Zátonyi, M. Madarász, Á. Szabó, T. Lőrincz, R. Hodován, B. Rózsa, Z. Fekete, Transparent, low-auto fluorescence microECoG device for simultaneous Ca^{2+} imaging and cortical electrophysiology in vivo, J. Neural. Eng. 17 (2020), 016062, https://doi.org/10.1088/1741-2552/ab603f.

[8] K.P. Prasad, Y. Chen, M.A. Sk, A. Than, Y. Wang, H. Sun, K.-H. Lim, X. Dong, P. Chen, Fluorescent quantum dots derived from PEDOT and their applications in optical imaging and sensing, MATERIALS HORIZONS 1 (2014) 529, https://doi.org/10.1039/c4mh00066h.

[9] A. Elschner, S. Kirchmeyer, W. Lövenich, U. Merker, K. Reuter, PEDOT - Principles and Applications of an Intrinsically Conductive Polymer, CRC Press, Taylor&Francis, Boca Raton, 2010, ISBN 9781420069112.

[10] E.S. Muckley, C.B. Jacobs, K. Vidal, J.P. Mahalik, R. Kumar, B.G. Sumpter, I. N. Ivanov, New insights on electro-optical response of poly(3,4-ethylenedioxythiophene):poly(styrenesulfonate) film to humidity, ACS Appl. Mater. Interfaces 9 (2017) 15880, https://doi.org/10.1021/acsami.7b03128.

[11] G. Márton, I. Bakos, Z. Fekete, I. Ulbert, A. Pongrácz, Durability of high surface area platinum deposits on microelectrode arrays for acute neural recordings, J. Mater. Sci. Mater. Med. 25 (2014) 931, https://doi.org/10.1007/s10856-013-5114-z.

[12] N. Bhagwat, K.L. Kiick, D.C. Martin, Electrochemical deposition and characterization of carboxylic acid functionalized PEDOT copolymers, J. Mater. Res. 29 (23) (2014) 2835, https://doi.org/10.1557/jmr.2014.314.

[13] K. Wagner, J.M. Pringle, S.B. Hall, M. Forsyth, D.M. MacFarlane, D. L Officer, Investigation of the electropolymerisation of EDOT in ionic liquids, Synth. Met. 153 (2005) 257, https://doi.org/10.1016/j.synthmet.2005.07.266.

[14] A.P. Sandoval, J.M. Feliu, R.M. Torresi, M.F. Suárez-Herrer, Electrochemical properties of poly-(3,4-ethylenedioxythiophene) grown on Pt(111) in imidazolium ionic liquids, RSC Adv. 4 (2014) 3383, https://doi.org/10.1039/c3ra46028b.

[15] K. Cysewska (nee Włodarczyk), J. Karczewski, P. Jasiński, Influence of electropolymerization conditions on the morphological and electrical properties of PEDOT film, Electrochim. Acta 176 (2015) 156, https://doi.org/10.1016/j.electacta.2015.07.006.

[16] M. Suominen, P. Damlin, C. Kvarnström, Electrolyte effects on formation and properties of PEDOT-graphene oxide composites, Electrochim. Acta 307 (2019) 214, https://doi.org/10.1016/j.electacta.2019.03.157.

[17] I. Ivanko, J. Pánek, J. Svoboda, A. Zhigunov, E. Tomšík, Tuning the photoluminescence and anisotropic structure of PEDOT, J. Mater. Chem. C 7 (2019) 7013, https://doi.org/10.1039/c9tc00955h.

[18] G. Mészáros, C. Li, I. Pobelov, T. Wandlowski, Current measurements in a wide dynamic range - applications in electrochemical nanotechnology, Nanotechnology 18 (42) (2007) 424004, 8.

[19] B.E. Conway, Ch. 3 in ELECTROCHEMICAL SUPERCAPACITORS, Scientific Fundamentals and Technological Applications, Kluwer Academic/Plenum Publishers, New York, 1999, ISBN 0306457369.

[20] A.J. Bard, L.R. Faulkner, Chapter 5, in: ELECTROCHEMICAL METHODS, Fundamentals and Applications, second ed., John Wiley & Sons, Inc, New York, 2001.

[21] C.P. Andrieux, P. Audebert, Electron transfer through a modified electrode with a fractal structure: cyclic voltammetry and chronoamperometry responses, J. Phys. Chem. B 105 (2001) 444, https://doi.org/10.1021/jp001565k.

[22] M.D. Levi, R. Demadrille, A. Pron, M.A. Vorotyntsev, Y. Gofer, D. Aurbach, Application of a novel refinement method for accurate determination of chemical diffusion coefficients in electroactive materials by potential step technique, J. Electrochem. Soc. 152 (2) (2005) E61, https://doi.org/10.1149/1.1851033.